https://doi.org/10.5194/angeo-2023-1
Preprint. Discussion started: 12 January 2023
© Author(s) 2023. CC BY 4.0 License.

Annales Geophysicae Discussions

Parallel electric fields produced by the ionospheric injection

Office Geophysik, Ogoori, 838-0141, Japan
Osuke Saka
saka.o@nifty.com

Abstract
It is well known that there exists a thin layer in lower boundary of the ionosphere between altitudes of 80 km and 140 km in which collisional ions and collisionless electrons mix. Local breakdown of charge neutrality may be initiated in this layer by electric fields from the magnetosphere as well as by electric fields generated there by the local neutral winds. The breakdown may be momentarily canceled by the Pedersen currents, but a complete neutralization is prevented because some ionospheric plasmas are released as outflows by parallel electric fields. Those parallel electric fields are produced by inherent plasma processes in the polar ionosphere and act as auroral drivers in the topside ionosphere.

1. Introduction

The closure of field-aligned currents (FAC) transmits the Poynting flux of the fields and particle momentum to the Earth's ionosphere, which in turn generates parallel electric fields for particle precipitation [Block, 1977]. These parallel electric fields associated with the FAC contribute to auroral radiance as well as the outflow of atmospheric ions [Seki et al., 2003; Moore and Holwitz, 2007; Engwall, 2009; Strangeway et al., 2010; Birn et al., 2012]. Vortical plasma motions in the equatorial plane, such as that associated with transient enhancement of magnetospheric convection and fast earthward flows (BBF) from the magnetotail, provide a source of FAC in the magnetosphere [Kan et al., 1982; Birn et al., 2004]. The ionosphere generally contains currents supplied from the magnetosphere; current continuity in the ionosphere via the FAC requires constitution of the electrostatic potential in the ionosphere, which in turn produces currents in the ionosphere via electric fields [Kamide and Matsushita, 1979].

In contrast, the ionosphere has the capability to produce electrostatic potential itself through differences in the mobility of collisional ions and collisionless electrons once the electric fields are transmitted along field lines into the auroral zone from the magnetosphere

https://doi.org/10.5194/angeo-2023-1
Preprint. Discussion started: 12 January 2023
© Author(s) 2023. CC BY 4.0 License.

Annales Geophysicae
Discussions

or produced there by the local neutral winds. In the E region, these electric fields may accumulate collisionless electrons in one direction, while collisional ions cannot follow them. The electrostatic potential thus produced in the E region generates parallel potentials to sustain original potential structures. In this scenario, Poynting fluxes propagated along the field lines would finally dissipate in the ionosphere by driving the ionospheric Pedersen currents closed through the FACs. The present scenario fits the MI-coupling caused by the parallel electric fields along the field lines, while the FACs are not the primary component of the coupling. The proposed new scenario referred to as ionospheric injection is summarized in Sect. 2. Summary and discussion are presented In Sect. 3.

2. Ionospheric injection

We consider cases where negative potential regions are produced by the local breakdown of the charge neutrality. The breakdown occurred in a thin layer located at boundaries between mesosphere and thermosphere where collisional ions and collisionless electrons mix [Rishbeth and Garriot, 1969]. The thin layer distributes at altitude of 140 km to 80 km and is referred to as ionosphere hereafter. Negative charges in the negative potential regions yield vertical component of electric fields (downward) above the ionosphere. If the vertical fields were of the order of $100\mu V/m$, the force associated with the electric fields and the force arising from the magnetic mirror force on the hot electrons ($T_e = 1keV$) are comparable. The downward electric fields displace the mirror point of the hot plasmas (electrons) supplied from the tail to higher altitudes. Ions do not change their pitch angle because ions that moved mirror point to lower altitudes enter the loss cone. Following Persson (1963), we assume that disagreed angular distributions of ions and electrons at each point produce space charges in the flux tube and integration of them along the field lines generates parallel electric fields.

Distribution of the pitch angle along the field lines can be expressed using constant of the motion,

$$\mu = \frac{m_q}{2B} v^2 \sin^2 \alpha .$$

Here, α denotes pitch angle at the magnetic field *B*, and $m_q v^2/2$ is kinetic energy of particle *q* conserved along the field lines. Substituting B_R at the mirror height ($\sin^2 \alpha = 1$), altitude profiles of the pitch angle above the reflection point can be given as,

$$\sin^2 \alpha = \frac{B}{B_R} .$$

https://doi.org/10.5194/angeo-2023-1
Preprint. Discussion started: 12 January 2023
© Author(s) 2023. CC BY 4.0 License.

Figure 1 shows altitude profile of $\sin^2\alpha$ along L=6 of the dipole fields from the ionosphere to 10,520 km above it. The black line denotes $\sin^2\alpha$ for ions and the red line is for electrons. It is assumed that electron mirror height ($\sin^2\alpha = 1$) moves to 1,226 km above the ionosphere (X=0.54 Re) where field magnitude is 60% of that at the ionospheric altitudes, while ions did not change their mirror height at the ionosphere (X=0.42 Re). Disagreed pitch angle distributions between electrons and ions along the field lines result in discrepancies in the number densities of electrons and ions at each point. The number density difference reaches a maximum when populations in the loss cone are empty. When the loss cone contains full populations, density difference becomes null.

The number densities of hot plasmas are calculated substituting isotropic Maxwellian distribution of temperature T_q,

$$f_{trap}(v_{//}, v_\perp) = \left(\frac{m_q}{2\pi k T_q}\right)^{3/2} \exp\left(-\frac{m_q}{2kT_q}\left(v_{//}^2 + v_\perp^2\right)\right) \text{ out of the loss cone, and}$$

$$f_{loss}(v_{//}, v_\perp) = \alpha f_{trap}(v_{//}, v_\perp) \text{ in the loss cone}$$

into

$$\frac{n_q}{n_0} = 2\pi \int \left[f_{trap}(v_{//}, v_\perp) + f_{loss}(v_{//}, v_\perp) \right] v_\perp dv_\perp dv_{//} .$$

Here, q is applicable to either electrons or ions. Note that $\alpha < 1$ to reduce populations in the loss cone.

We choose two cases; phase space density in loss cone is reduced to half of the trapped ones ($\alpha = 0.5$) and empty ($\alpha = 0$).

Normalized density difference, $(n_i - n_e)/n_0$, associated with pitch angle curves in Figure 1 is shown in Figure 2, where loss cone is assumed to be empty ($\alpha = 0$). When we choose $\alpha = 0.5$, normalized density difference shown in Figure 2 was reduced to half.

In the one-dimensional model, parallel electric fields at s_1 are calculated by integrating the density difference along field lines s,

$$E_{//}(s_1) = \int_{s_0}^{s_1} \frac{e(n_i - n_e)}{\varepsilon_0} ds .$$

Here s_0 denotes ionospheric altitude where integration starts. These are plotted in Figure 3 starting from the ionosphere (0 km) to a point 10,520 km. To plot profiles of the parallel electric fields in Figure 3, geometrical factor ($\sqrt{B_{s_1}/B_{s_0}}$) was multiplied to $E_{//}(s_1)$ for adjusting the diverging geometry of the dipole configuration. $E_{//}(s_1)$ is linearly proportional

https://doi.org/10.5194/angeo-2023-1
Preprint. Discussion started: 12 January 2023
© Author(s) 2023. CC BY 4.0 License.

to the background hot plasma density supplied from the tail. In this plot, hot plasma density $n_0 = 10^{-1} m^{-3}$ was assumed. Two cases are plotted in Figure 3: (A) hot plasma populations empty in the loss cone and (B) population in the loss cone filled with half of the trapped plasma density. In each figure, new mirror points of hot electrons are (a) 1,226 km, (b) 240 km, and (c) 119 km above the ionosphere where the field magnitudes were 60%, 90%, and 95% of those at the ionosphere, respectively. Note that the electric field intensity in Figure 3(B) was reduced to half for all cases in Figure 3(A). These are non-vanishing parallel electric fields along the field lines created by the discrepant pitch angle distributions of ions and electrons at each point [Persson, 1963]. The parallel electric fields started from the ionosphere have a peak at 2,000 - 3,000 km and decrease monotonically with altitudes because of the diverging effect of the flux tubes. Figure 4 depicts electrostatic potential profiles obtained by integrating parallel electric fields of (a), (b), and (c) in Figure 3(A) along field lines.

3. Discussion and Summary

It is shown that breakdown of charge neutrality in the polar ionosphere resulted in disagreement of angular distributions of ion and electron velocities which in turn generated parallel electric fields above the ionosphere with peak amplitudes at 3,000 km. Those electric fields decreased monotonically to the equatorial plane. Normally, the local breakdown would be triggered by the transverse electric fields transmitted from the magnetosphere during the dipolarization onset. We can suggest that ionospheric injection may excite substorm auroras in polar ionosphere.

We also consider the cases where breakdown of the charge neutrality was initiated in the polar ionosphere by the neutral winds. If wind channel was localized along x between x_1 to x_2, neutral wind generates positive charge in leading edge (x_2) and negative charge in trailing edge (x_1); the ExB drift (E is polarization electric fields in the wind channel) generates negative charge to one side and positive to the other side of the wind channel. Auroras are produced at the negative charge region as spiral auroras. If wind velocity is weaker than ExB drift, breakdown of the charge neutrality may not happen because polarization drift of ions suppressed the charging up of the ionosphere. Wind velocities of the order of $10^3 m/s$ are necessary to produce substorm auroras by the neutral wind. This scenario may be reminiscent of auroras among gas planets in the solar system such as weather-driven auroras in Saturn [Chowdhury et al., 2021].

https://doi.org/10.5194/angeo-2023-1
Preprint. Discussion started: 12 January 2023
© Author(s) 2023. CC BY 4.0 License.

4. Data availability

No data sets were used in this article.

5. Competing interest

The author declares that there is no conflict of interest.

https://doi.org/10.5194/angeo-2023-1
Preprint. Discussion started: 12 January 2023
© Author(s) 2023. CC BY 4.0 License.

References

Birn, J., Raeder, J., Wang, Y.L., Wolf, R.A., and Hesse, M.: On the propagation of bubbles in the geomagnetic tail, Ann.Geophys., 22, 1773-1786, 2004.

Birn, J., Artemyev, A.V., Baker, D.N., Echim, M., Hoshino, M., and Zelenyi, L.M.: Particle acceleration in the magnetotail and aurora, Space Sci. Rev., 173, 49-102, 2012.

Block, L.P.: Double layer review, Tech. Rep. TRITA-EPP-77-16, Dep. Plasma Phys., Roy. Insti. of Technol., Stockholm, Sweden, 1977.

Engwall, E.: Low-energy ion escape from the terrestrial polar regions, Acta Universitatis Upsaliensis. Digital Comprehensive Summaries of Upsala Dissertations from the Faculty of Science and Technology 640. 91 pp. Uppsala. ISBN 978-91-554-7512-3, 2009.

Chowdhury, N.M., Stallard, T.S., Baines, K.H., Provan, G., Melin, H., Hunt, J.G., Moore, L., O'Donoghue, J., Thomas, E.M., Wang, R., Miller, S., and Badman, S.V.: Saturn's weather-driven aurorae modulate oscillations in the magnetic field and radio emissions, Geophys. Res., Lett., 49, e2021GL096492, 2021.

Kamide, Y., and Matsushita, S.: Simulation studied of ionospheric electric fields and currents in relation to field-aligned currents, 1. quiet periods, J. Geophys. Res., 84, 4083-4098, 1979.

Kan, J.R., Longenecker, D.U., and Olson, J.V.: A transient response model of Pi2 pulsation, J.Geophys.Res., 87, 7483-7488, 1982.

Moore, T.E., and Horwitz, J.L.: Stellar ablation of planetary atmospheres, Rev.Geophys, 45, doi:10.1029/2005RG000194, 2007.

Persson, H.: Electric field along a magnetic line of force in a low-density plasma, Physics Fluids, 6, 1756-1759, 1963.

Rishbeth, H., and Garriott, O.K.: Introduction to ionospheric physics, International Geophysics, 14, 1-331, 1969.

Saka, O.: Ionospheric control of space weather, Ann. Geophys. 39, 455-460, 2021.

Seki, K., Hirahara, M., Hoshino, M., Terasawa, T., Elphic, R.C., Saito, Y., Mukai, T., Hayakawa, H., Kojima, H., and Matsumoto, H.: Cold ions in the hot plasma sheet of Earth's magnetotail, NATURE, 442589-592, 2003.

Strangeway, R.J., Russell, C.T., and Luhmann, J.G.: Comparative planetorogy: How effective is an intrinsic magnetic field in shielding a planetary atmosphere?, EPSC abstract, 5, EPSC2010-334, 2010.

https://doi.org/10.5194/angeo-2023-1
Preprint. Discussion started: 12 January 2023
© Author(s) 2023. CC BY 4.0 License.

Annales Geophysicae Discussions Open Access EGU

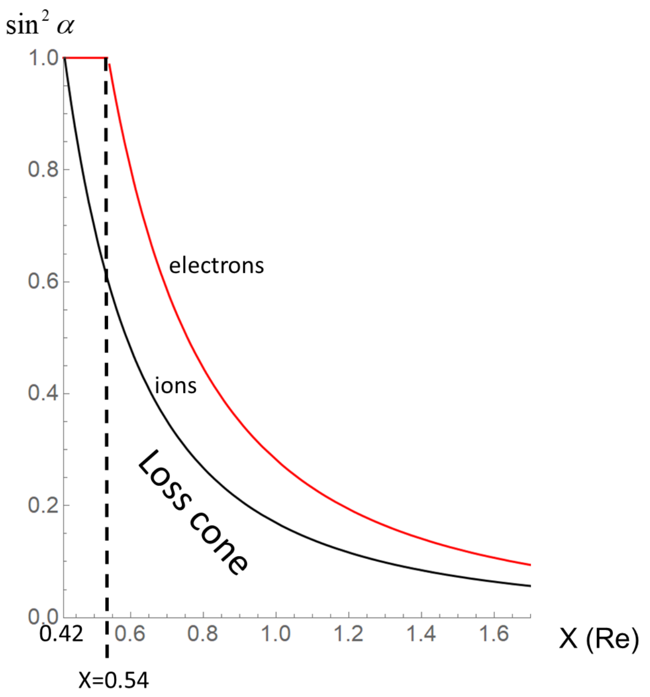

Figure 1

203 Altitude profiles of $\sin^2\alpha = B/B_R$ for electrons (red) and ions (black). X (Re) denotes equatorial projection of the altitudes, from the ionosphere (X=0.42 Re) to 10,520 km above it (X=1.70 Re). B_R represents field magnitudes of mirror point. Mirror point for ions is at the ionosphere. Electrons moved their mirror point to higher altitudes at 1,226 km above the ionosphere (X=0.54 Re). In loss cone, plasmas are empty or filled with reduced populations (see text).

https://doi.org/10.5194/angeo-2023-1
Preprint. Discussion started: 12 January 2023
© Author(s) 2023. CC BY 4.0 License.

Annales Geophysicae Discussions Open Access

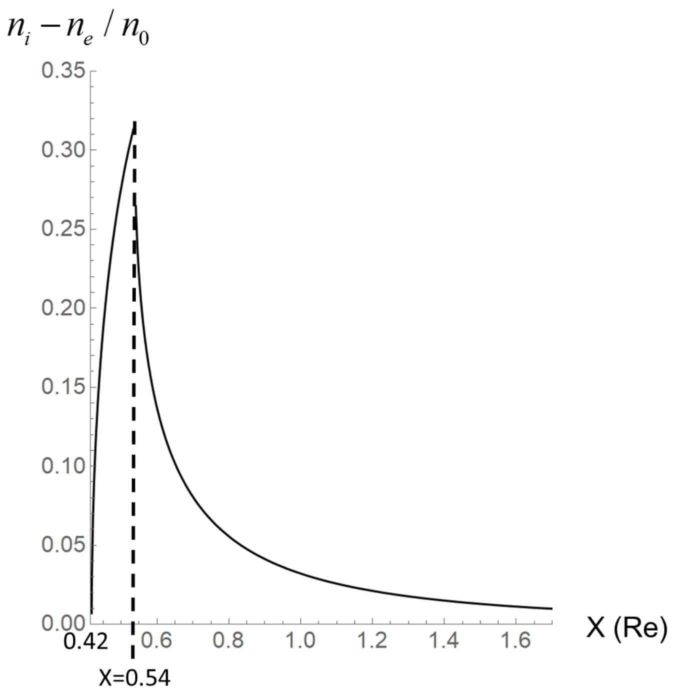

Figure 2

Difference of number density $n_i - n_e$ normalized by n_0. Number densities of ions (n_i) and electrons (n_e) are calculated by integrating Maxwellian distribution over velocity space. Plasma density in loss cone is empty. The plot along L=6 started from the ionosphere (X=0.42 Re) to 10,520km above it (X=1.70 Re). Real density is given by multiplying n_0. Density gap at X=0.54 Re is caused by discontinuous change of $\sin^2\alpha$.

https://doi.org/10.5194/angeo-2023-1
Preprint. Discussion started: 12 January 2023
© Author(s) 2023. CC BY 4.0 License.
Annales Geophysicae Discussions Open Access EGU

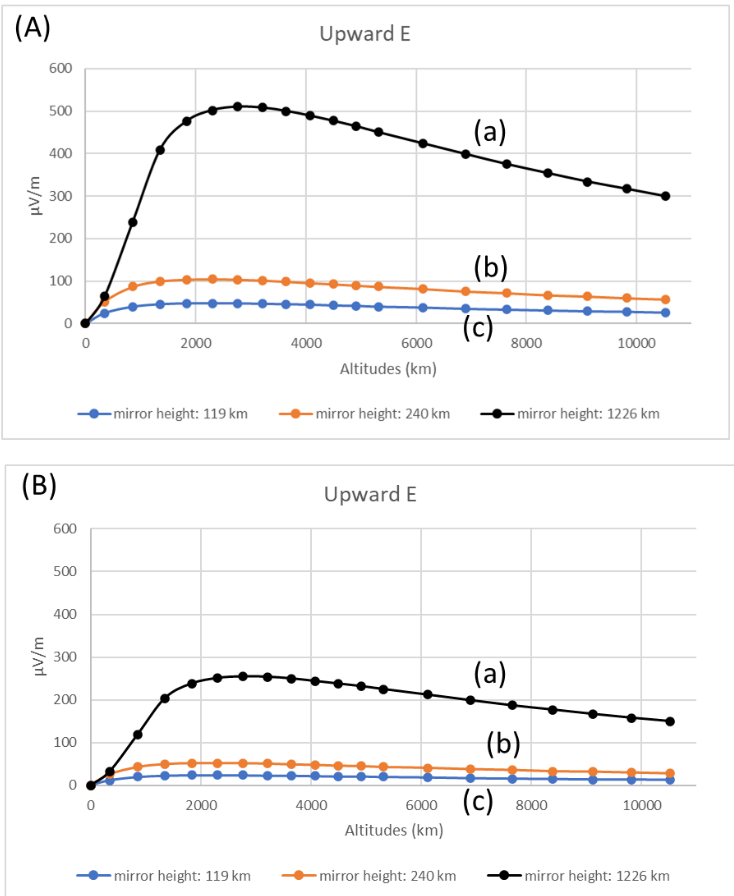

Figure 3

Altitude profiles of parallel electric fields $E_{//}$ (upward, $\mu V/m$) along field lines. Horizontal axis is altitudes in km of the field lines along L=6. Note that the ionosphere is at 0 km. (A) plasma density in loss cone is empty. (B) density is reduced in loss cone to 50% of the trapped populations. New mirror point was (a) 1,226 km, (b) 240 km, and (c) 119 km above the ionosphere for (A) and (B).

https://doi.org/10.5194/angeo-2023-1
Preprint. Discussion started: 12 January 2023
© Author(s) 2023. CC BY 4.0 License.

Annales Geophysicae
Discussions
Open Access

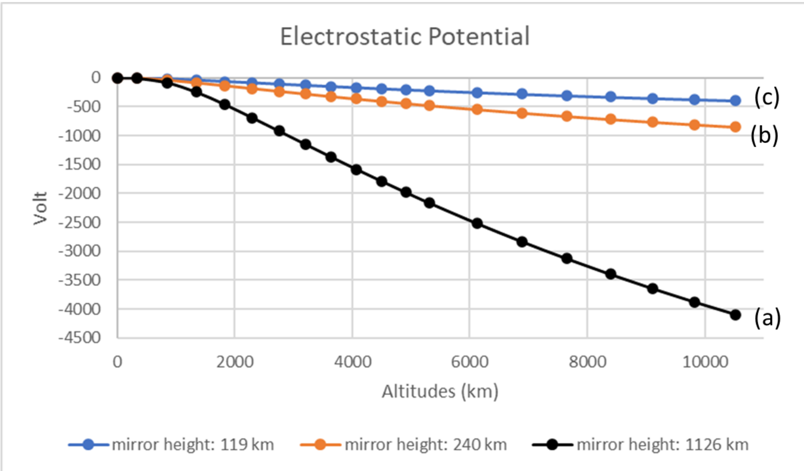

Figure 4

219 Altitude profiles of electrostatic potentials (Volt) of flux tubes from the ionosphere to 10,520 km. Parallel electric fields marked (a), (b), and (c) in Figure 3(A) were integrated along field lines to plot potential profiles (a), (b), and (c) in the figure, respectively. Electrostatic potential is assumed to be zero at the ionosphere.